

Prospects for detecting Gamma-Ray Bursts with the Cherenkov Telescope Array

T. Di Girolamo^{a,b}, E. Bissaldi^{c,d}, F. Di Pierro^e, T. Gasparetto^f, F. Longo^{f,g}, P. Vallania^{e,h}, C. F. Vigorito^{h,i}, for the CTA Consortium^j

^aUniversità degli Studi di Napoli “Federico II”, Napoli, Italy

^bIstituto Nazionale di Fisica Nucleare, Sezione di Napoli, Napoli, Italy

^cIstituto Nazionale di Fisica Nucleare - Sezione di Bari, Bari, Italy

^dPolitecnico di Bari, Bari, Italy

^eIstituto Nazionale di Astrofisica, Osservatorio Astrofisico di Torino, Torino, Italy

^fUniversità degli Studi di Trieste, Trieste, Italy

^gIstituto Nazionale di Fisica Nucleare, Sezione di Trieste-Udine, Trieste, Italy

^hIstituto Nazionale di Fisica Nucleare, Sezione di Torino, Torino, Italy

ⁱUniversità degli Studi di Torino, Torino, Italy

^jSee www.cta-observatory.org for full author and affiliation list

Abstract

The Large Area Telescope (LAT) on the Fermi gamma-ray satellite telescope observes Gamma-Ray Bursts (GRBs) at energies above 100 MeV. Thanks to a new detection algorithm and a new event reconstruction, it is expected to publish a catalogue with more than 100 GRBs. This work aims at revising the prospects for GRB alerts with the Cherenkov Telescope Array (CTA) based on the new LAT results. We start by considering the simulation of the observations with the full CTA of two extremely bright events, the long GRB 130427A and the short GRB 090510; then we investigate how these GRBs would be observed by different subsamples of the array pointing to different directions, adopting the “coupled divergent” mode.

Keywords: Cherenkov telescopes, High-energy gamma rays, Gamma-ray bursts

1. CTA configurations

The Cherenkov Telescope Array (CTA) is a worldwide project aiming at building and operating the next generation of Imaging Atmospheric Cherenkov Telescopes (IACTs). In its present design, CTA will consist of two arrays for a total of more than 100 telescopes, one in the Southern (Paranal, Chile) and one in the Northern (La Palma, Spain) hemisphere. In order to cover the energy range from 20 GeV to more than 100 TeV, the following three different kinds of telescopes are envisaged, each driven by the features of the Cherenkov signal at different energies.

Large Size Telescopes (LSTs), with a diameter of 23

m, will observe the 20–200 GeV energy region, having a compact placement in both Northern and Southern sites (each with 4 telescopes). Near the energy threshold, the number of source photons is relatively high but the Cherenkov image is poor, therefore a few huge telescopes are used to collect faint showers.

Medium Size Telescopes (MSTs), with a diameter of 12 m, will be sensitive in the 100 GeV–10 TeV range, scattered on an area of about 3 km² (15 telescopes in the Northern site and 25 in the Southern one). At these energies, the Cherenkov signal starts to increase while the source flux rapidly fades, so an intermediate choice for number and dimensions of the telescopes is optimal.

Small Size Telescopes (SSTs), with a diameter of 4 m, will operate in the 5–300 TeV interval, covering an area of about 6–7 km² (70 telescopes only in the Southern site, where most of the Galactic plane is visible).

Email address: tristano.digirolamo@na.infn.it (T. Di Girolamo)

At the highest energies, the Cherenkov signal is very strong, however the steep source spectra reduce the signal to a few primary gamma-rays.

2. High-energy GRB observations

Due to their elusive nature, GRBs represent a very interesting candidate for future observations by CTA [1, 2]. Most of the previous prospect analyses relied on extrapolations taken from: (1) the GRB spectral parameters published in the catalogs of the Burst And Transient Source Experiment (BATSE, 20 keV–2 MeV) or of the Swift Burst Alert Telescope (BAT, 15–150 keV); (2) some very energetic GRBs detected by the Fermi gamma-ray satellite telescope before 2012.

Since June 2008, the Fermi satellite is constantly enhancing the number of GRB detections. The field of view of the Fermi Gamma-ray Burst Monitor (GBM, [3]) is almost 4π sr, for a trigger rate of ~ 250 GRB/yr (higher than the ~ 100 GRB/yr of BAT). Furthermore, thanks to the other detector on board Fermi, the Large Area Telescope (LAT) [4], the number of high-energy GRBs dramatically increased with respect to the bunch of events detected in the '90s by the Energetic Gamma-Ray Experiment Telescope (EGRET, 20 MeV–30 GeV).

The current number of official LAT GRB detections is constantly updated on the LAT Public Table website [5] and lists almost 120 GRBs at the time of this writing, that is, after eight years into the Fermi mission. However, this number is meant to grow with the new event reconstruction algorithm (the so-called *Pass 8*).

The GRB sample which we consider is made by the three following Fermi catalogs:

- a) the second Fermi GBM GRB catalog [6], with about 1000 GRBs observed during 4 yr in the energy range 8 keV–40 MeV;
- b) the first Fermi LAT GRB catalog [7], with 35 GRBs observed during 3 yr in the region 30 MeV–300 GeV;
- c) the second Fermi-LAT GRB catalog [8], with about 100 GRBs observed during 6 yr in the interval 30 MeV–300 GeV.

This work focuses on Fermi-like GRBs (both prompt and late-time emissions) with measured redshift, aiming at setting up a library of GRBs observed at different epochs after the trigger, obtained by studying the extrapolation of the LAT flux to higher energies, taking into account its temporal evolution. For this contribution, we use as test cases two very bright GRBs with redshift, one long (GRB 130427A) and one short (GRB 090510).

3. Effect of the EBL

The interaction of extragalactic Very High Energy (VHE) photons with the Extragalactic Background Light (EBL) at optical-UV wavelengths produces an e^+e^- pair and thus an exponential attenuation of the gamma-ray flux. This absorption increases with the source redshift, the gamma-ray energy and the photon density of the EBL (for a review, see [9]), strongly depressing the high-energy spectra of distant sources detected at Earth. Many EBL models have been published in the last decades, with a general trend towards a decrease of the corresponding optical depth due to the observation of VHE photons at larger redshifts, which were recently detected from blazars at $z \simeq 1$ [10, 11, 12]. The EBL models are getting close to the firm lower limits derived from integrated galaxy number counts [13]. As an indication, the high-energy spectrum of a source at $z \simeq 1$ shows a cutoff at $E \simeq 100$ GeV. In our work, we adopt the EBL model by [14] and, for simplicity, in our simulations we extend the spectrum only up to 1 TeV, the maximum energy after which the source is assumed to be totally absorbed.

However, the observed spectral indices in blazars do not seem to follow the amount of softening with increasing redshift predicted by the EBL absorption, and a possible explanation could be the oscillation from photons to Axion-Like Particles (ALPs), which propagate unimpeded over cosmological distances before reconversion, reducing the optical depth along the VHE gamma-ray path [15]. In this framework, GRBs, with their cosmological distances (mean redshift $z \simeq 2$), may be useful to add stronger constraints on the EBL and to give new hints to the potential existence of ALPs.

The effect of the EBL absorption is included only in the simulations of GRB 130427A.

4. Simulations of GRB observations with *ctools*

In order to estimate the detectability of a GRB, we use *ctools* (v0.9.0), a software package specifically developed for the scientific analysis of CTA data [16].

In the first test case, we simulate the high-energy emission of the long, extremely fluent, GRB 130427A, at redshift $z = 0.34$, as observed by LAT, with spectral index $\gamma = -2.2$ (almost constant from 400 s up to 70 ks after the trigger) and a power law decay with temporal index $\tau = -1.35$ (valid for $t > 380$ s) [17] (see Figure 1). The GRB is simulated in the 50 GeV–1 TeV energy range, assuming observations on axis with respect to the CTA array and a zenith angle $\theta = 20^\circ$. The

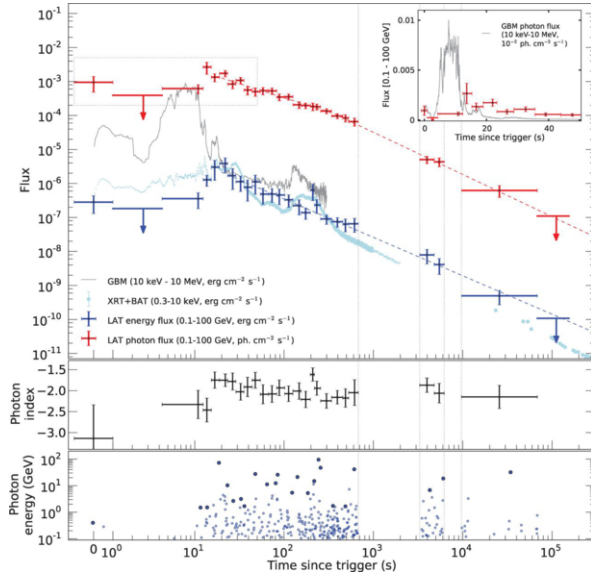


Figure 1: Temporally extended LAT emission of GRB 130427A (taken from [17]).

Instrument Response Functions (IRFs) *North_0.5h* and *North_5h* are adopted [18].

In the second test case, we simulate the high-energy emission of the short, bright, GRB 090510, at $z = 0.9$, with spectral and temporal indices $\gamma = -1.6$ (for $t \leq 200$ s); $\gamma = -2.5$ (for $t > 200$ s) and $\tau = -1.38$, respectively [19, 20] (see Figure 2). The *ctools* input parameters are the same as for GRB 130427A, however, since the EBL absorption is not yet considered in this case, the energy range is limited to 50–100 GeV.

4.1. Results

We simulate two possible observations of GRB 130427A: (a) duration of 10 min starting from $t = 1$ ks after the trigger; (b) duration of 1 hr from $t = 10$ ks after the trigger. Figure 3 shows the two resulting count maps at different epochs. We find a significant detection in both cases.

For the short GRB 090510, we simulate two different observations: (a) duration of 100 s starting from $t = 100$ s after the trigger; (b) duration of 500 s from $t = 1$ ks after the trigger. Figure 4 shows the two resulting count maps. In case (b) the signal has almost vanished.

Further analysis is in progress, also to study the performance of the “coupled divergent mode” for CTA, in which couples of telescopes are pointing to slightly different positions, and the contribution of the MSTs in GRB searches.

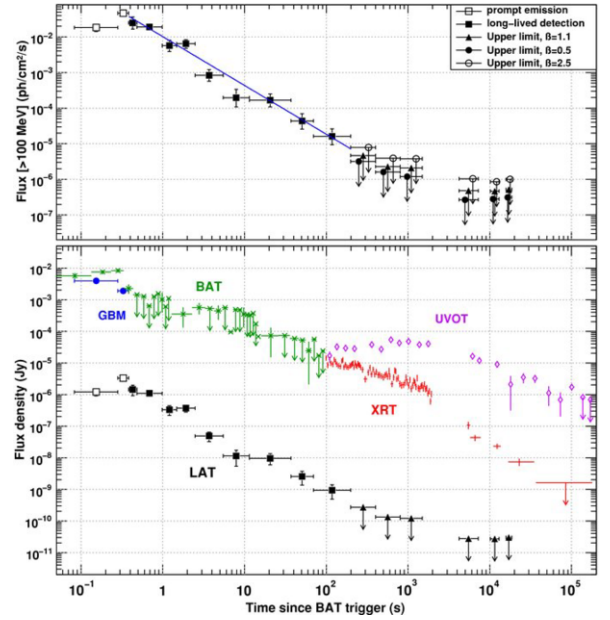


Figure 2: Light curve of GRB 090510 from Swift and Fermi observations (taken from [19]).

5. Acknowledgments

We gratefully acknowledge support from the agencies and organizations listed under Funding Agencies at this website: <http://www.cta-observatory.org/>.

References

- [1] S. Inoue et al., *Astropart Phys* **43** 252 (2013)
- [2] R. C. Gilmore et al., *Exp Astron* **35** 413 (2013)
- [3] C. Meegan et al., *ApJ* **702** 719 (2009)
- [4] W. B. Atwood et al., *ApJ* **697** 1071 (2009)
- [5] http://fermi.gsfc.nasa.gov/ssc/observations/types/grbs/lat_grbs/
- [6] A. von Kienlin et al., *ApJS* **211** 13 (2014)
- [7] M. Ackermann et al., *ApJS* **209** 11 (2013)
- [8] G. Vianello et al., *Proc. Fermi Symposium 2014*, (arXiv:1502.03122)
- [9] E. Dwek and F. Krennrich, *Astropart Phys* **43** 112 (2013)
- [10] R. Mirzoyan et al., *ATel* #6349 (2014)
- [11] R. Mirzoyan, *ATel* #7416 (2015)
- [12] R. Mukherjee, *ATel* #7433 (2015)
- [13] P. Madau and L. Pozzetti, *MNRAS* **312** L9 (2000)
- [14] A. Franceschini et al., *A&A* **487** 837 (2008)
- [15] A. De Angelis et al., *Phys Rev D* **84** 105030 (2011)
- [16] <http://cta.irap.omp.eu/ctools/index.html>
- [17] M. Ackermann et al., *Science* **343** 42 (2014)
- [18] <https://portal.cta-observatory.org/Pages/CTA-Performance.aspx>
- [19] M. De Pasquale et al., *ApJ* **709** L146 (2010)
- [20] M. Ackermann et al., *ApJ* **716** 1178 (2010)

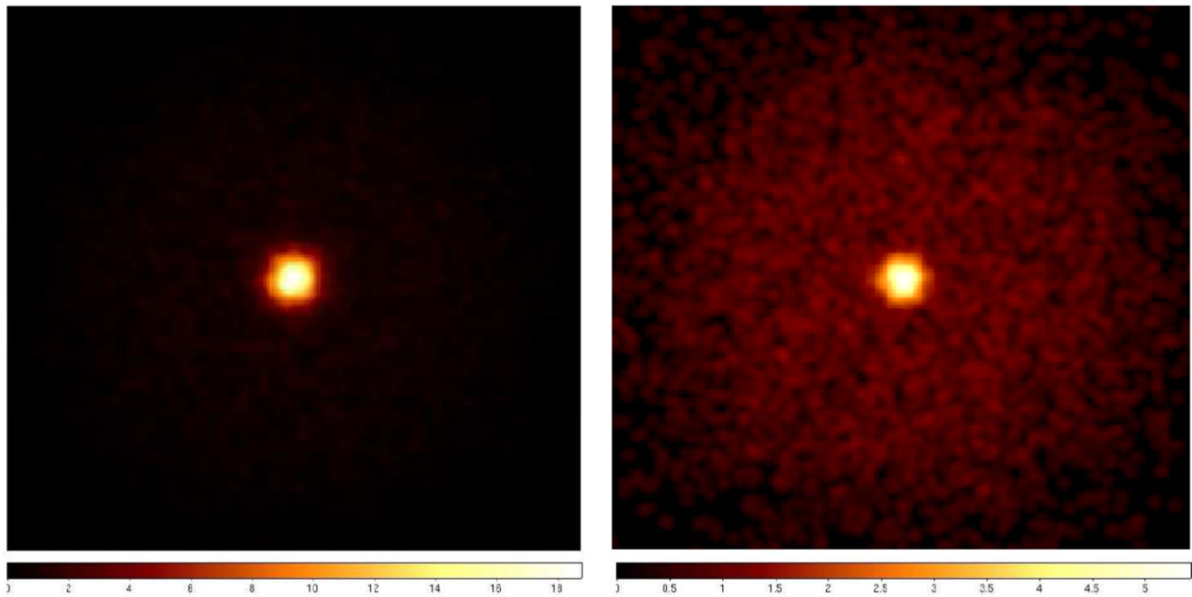


Figure 3: Simulations of GRB 130427A with *ctools* in the interval 50 GeV–1 TeV, considering the EBL absorption. The camera images are divided into 200×200 bins of 0.02° . The colour scale gives the counts/bin after Gaussian smoothing. *Left panel*: Count map as seen by CTA North in 10 min starting from 1 ks after the trigger. *Right panel*: Count map as seen by CTA North in 1 hr starting from 10 ks after the trigger.

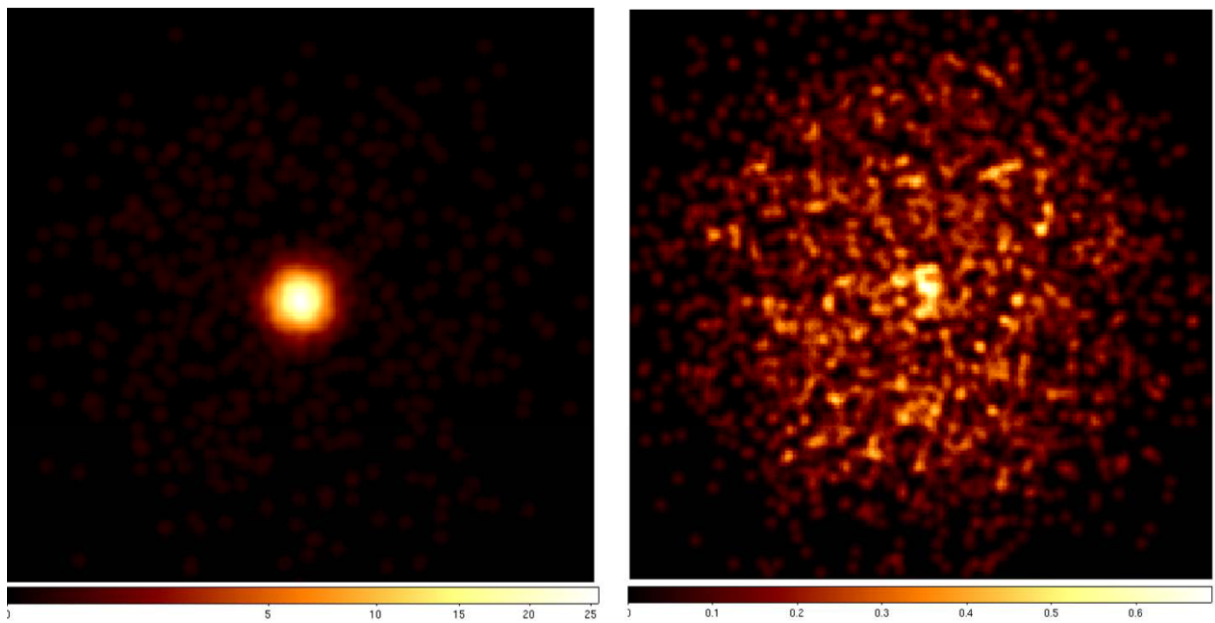


Figure 4: Simulations of GRB 090510 with *ctools* in the interval 50–100 GeV. The camera images are divided into 200×200 bins of 0.02° . The colour scale gives the counts/bin after Gaussian smoothing. *Left panel*: Count map as seen by CTA North in 100 s starting from 100 s after the trigger. *Right panel*: Count map as seen by CTA North in 500 s starting from 1 ks after the trigger.